

Dissecting Human Body Representations in Deep Networks Trained for Person Identification

Thomas M Metz, Matthew Q Hill, Blake Myers, Veda Nandan Gandhi, Rahul Chilakapati,
Alice J O’Toole

School of Behavioral and Brain Science, The University of Texas at Dallas, Richardson, Texas

Abstract—Long-term body identification algorithms have emerged recently with the increased availability of high-quality training data. We seek to fill knowledge gaps about these models by analyzing body image embeddings from four body identification networks trained with 1.9 million images across 4,788 identities and 9 databases. By analyzing a diverse range of architectures (ViT, SWIN-ViT, CNN, and linguistically primed CNN), we first show that the face contributes to the accuracy of body identification algorithms and that these algorithms can identify faces to some extent—with no explicit face training. Second, we show that representations (embeddings) generated by body identification algorithms encode information about gender, as well as image-based information including view (yaw) and even the dataset from which the image originated. Third, we demonstrate that identification accuracy can be improved without additional training by operating directly and selectively on the learned embedding space. Leveraging principal component analysis (PCA), identity comparisons were consistently more accurate in subspaces that eliminated dimensions that explained large amounts of variance. These three findings were surprisingly consistent across architectures and test datasets. This work represents the first analysis of body representations produced by long-term re-identification networks trained on challenging unconstrained datasets.

I. INTRODUCTION

In recent years, body identification algorithms that go beyond short-term re-identification have been developed for a variety of important applications (cf. for a review [41]). These algorithms are useful when the face is not visible or is not of sufficient quality to be identified. A strong focus in long-term re-identification has been on the problem of clothing change, (e.g., [1], [12], [16], [18], [24], [26], [30], [40], [41]). Increasingly, body identification models have begun to tackle long-term re-identification in unconstrained viewing environments (e.g., [18], [26], [30]). These models build on the expanding availability of datasets suitable for training body identification networks over a wide range of views and distances [3]. The body representations that result from such training are robust to changes in clothing, viewpoint, illumination, and distance.

Despite recent advances in body-based identification, work aimed at understanding body representations in identity-

This research is based upon work supported in part by the Office of the Director of National Intelligence (ODNI), Intelligence Advanced Research Projects Activity (IARPA), via [2022-21102100005]. The views and conclusions contained herein are those of the authors and should not be interpreted as necessarily representing the official policies, either expressed or implied, of ODNI, IARPA, or the U.S. Government. The U.S. Government is authorized to reproduce and distribute reprints for governmental purposes notwithstanding any copyright annotation therein.

trained deep networks is surprisingly limited. Our goal is to provide an in-depth analysis of the information encoded in representations that support long-term body identification. We consider three questions. First, how much does the face contribute to the performance of long-term body identification networks? This question has implications for the security and privacy of body identification models [7].

Second, do body recognition networks retain information about person attributes (gender) and about imaging conditions (camera angle, dataset of origin), in addition to identity? We will show that they do. The nature of information retained in body embeddings has implications for determining potential use cases for these models, including the development of semantic editing applications [36]. Third, can editing of the latent space improve identification performance without additional training?

We focus on the analysis of body representations in four identity-trained body networks with diverse backbone architectures (ResNet [13], Vision Transformer [8] and Swin Vision Transformer [27]). Different architectures were used to distinguish between coding principles common across networks and those that apply to specific architectures. We equated training across models to ensure that differences among model-generated representations would not be due to the training data. To achieve robust models with the most generalizable applicability, we compiled a large and diverse training dataset comprised of over 1.9 million images of nearly 5K identities across 9 datasets.

A. Contributions

- We show that identification accuracy declines when the head/face region is obscured in a whole-person image, indicating that the face contributes to body-identification.
- We show that networks trained for body identification are somewhat capable of face identification.
- Analogous to face identification networks, we show that body embeddings retain accurate information about a person’s gender and about the original image processed. The body viewpoint and originating dataset can be linearly decoded from the embedding.
- We show that identity comparisons made in the principal component space of deep network embeddings are consistently more accurate than those made on the raw embeddings.

- We show that it is possible to improve body identification accuracy by deleting parts of a network’s latent space. We propose a technique to remove subspaces that are not relevant for identification in real applications.

B. Background and Previous Work

1) Faces, bodies, and whole people in re-identification:

Face and body recognition are commonly treated as separate problems in computational vision. Reasons for this separation include differences in the expectation of uniqueness of faces versus bodies for identification, as well as differences in the quality and resolution of the image needed to recognize a face versus a body. In the real world, however, faces and bodies are seen together. As with humans, body identification models learn individual identities from images of whole people in the natural world. In the context of computation, body detection algorithms begin with an image of the whole person, including the face and head region. Thus, there is clear potential for the face/head to contribute to the performance of these algorithms.

Motivated by privacy concerns in re-identification, work to pinpoint the importance of face information in re-identification found only a minimal performance decrease when faces were blurred in the input image [7]. However, five of the six datasets tested in that work had no clothing change. It is possible, therefore, that clothing constancy compensated for the absence of a face. Here we re-examine the role of the face in long-term body identification algorithms tested with clothing-change datasets.

2) *Person and image attributes retained in body identification:* Face representations (embeddings) generated by deep networks trained to identify faces retain detailed information that is not useful for identification. Specifically, they retain information about “instances of encounter” in the form of image detail (e.g., viewpoint, illumination) [33], [15], [21], [37], expression [2], and appearance attributes (e.g., glasses, facial hair) [37]). Demographic categories, including gender, age, and race, are also retained [6], [15]. These attributes can be “read out” from the DNN-generated face code with simple linear networks [33], [6], [15], [34]. This type of “semantic” information in the latent space fuels the image-editing capabilities [36] inherent in face-trained generative adversarial networks (GANS) [11].

Semantic and image-based codes in the latent space of body identification networks have not been investigated. As for faces, we might expect coding of demographic information such as gender, as well as information based on image properties that result from camera angle and environment. We explore whether these semantic and image-based attributes can be classified from body image embeddings.

3) *Subspace representations can improve identification:*

Applications of person identification networks often rely on raw embeddings. However, prior to the deep network era, modifying image representations to improve identification performance was not uncommon. Numerous applications in early facial recognition showed that subspaces of facial image representations yield features that are more effective

at identification than complete representations (e.g., [32], [9], [43]). Dimensionality reduction in engineering nearly always refers to the deletion of PCs that explain small amounts of variance. However, information useful for uniquely identifying a person should be features that *are not shared with other identities* (i.e. information that explains small amounts of variance in a set of faces). In older image-based face recognition models, deletion of PCs that explain larger amounts of variance increased identification accuracy [32]. We explore this principle with deep network body identification models. At a more basic level, work prior to deep networks showed that performing a simple PCA on image representations increased retrieval performance [19]. Other modern work in person identification also uses representation subspaces for identification. For example, by constructing multi-modal representations, it is possible to find subspaces that improve identity discrimination [10]. Here, we consider the question of whether simple, non-augmented representation transformations can boost identification performance for deep networks trained for person re-identification.

II. METHODS

We focus on four models. Two of these are ResNet-based CNNs [13] and two are Vision Transformers [8], [27]. In what follows, we describe the model backbones and training. The core training data (Table I) and training methods described for the BIDDS model were used for all models, except where noted. All models were fit with a custom classification head mapped to a 2048-dimensional output space.

A. Models and Training

1) *Body Identification with Diverse Datasets (BIDDS):*

The BIDDS model was built on a Vision Transformer architecture, using a ViT-B/16 variant pre-trained on ImageNet-1k. The core model processes 224×224 pixel images with patch size 16. All models were trained to map images of bodies to identities (see Table I). Traditional re-id datasets like Market1501 [45] and MSMT17 [38] are included, as well as challenging long-term re-identification clothes-change datasets like DeepChange [39] and the BRIAR Research Dataset (BRS) [3]. The training data include a range of distances, camera angles, and weather conditions.

Hard triplet loss with negative mining [14] was used for training. This operates on image triplets: an anchor image, a positive sample (same identity), and a negative sample (different identity). The loss calculation measures the Euclidean distances between the anchor and positive samples and between the anchor and negative samples. We selected the most challenging negative samples (i.e., those closest to the anchor in the embedding space) within each batch. This hard negative mining encourages the model to learn features that effectively differentiate between similar body shapes. We used the Adam optimizer and incorporated dynamic sampling, whereby triplet selection is adapted based on the current state of the embeddings. This ensures that the model continuously encounters challenging examples throughout

training [20]. The training process employs a low learning rate (10^{-5}) and weight decay (10^{-6}) to prevent over-fitting while maintaining stability.

Following core training, the BIDDS model was fine-tuned on the BRS1–5 datasets (cf. [3]), increasing input resolution to 384×384 pixels.

2) *Swin Transformer Body Identification with Diverse Datasets (Swin-BIDDS)*: Swin-BIDDS utilizes the hierarchical vision transformer, which uses shifted windows [28]. This transformer is more efficient, because it limits self-attention computation to non-overlapping local windows, while supporting cross-window connections. The hierarchical structure progressively merges patches and is well-suited to modeling at various scales. We used an ImageNet-1k pretrained version of the model. The model was core trained (see Section II-A.1) with input resolution at 384×384 pixels. Swin-BIDDS fine-tuning was identical to BIDDS fine-tuning (see Section II-A.1).

3) *Linguistic Core ResNet Identity Model (LCRIM)*: LCRIM incorporates human body descriptors into its training.¹ A ResNet-50 model pretrained on ImageNet-1k [35] was used as a base. The base was augmented with an encoder/decoder structure that maps to a linguistic feature space before the final identification layers. The encoder pathway compresses the representation ($2048 \rightarrow 512 \rightarrow 64 \rightarrow 16$), while the decoder pathway ($16 \rightarrow 24 \rightarrow 30$) reconstructs linguistic body attributes. LCRIM was pretrained to produce body descriptors on the HumanID [31] and MEVA [4] datasets. HumanID consists of videos of 297 identities filmed from multiple angles, viewpoints, and lighting conditions. Subjects are filmed wearing different clothing sets. The MEVA dataset, comprising over 9,300 hours of video across varied activities and scenarios, contributed an additional 158 identities. Identities were annotated by 20 subjects for 30 human descriptors (e.g., broad shoulders, feminine, hourglass, long legs, pear-shaped, petite; for a full list, see [30]). Images from these datasets were used to train LCRIM’s initial ability to map between visual features and linguistic body descriptions.

The linguistic-core training was followed by a core training identical to that described in Section II-A.1. There was no additional fine-tuning.

4) *Non-Linguistic Core ResNet Identity Model (NLCRIM)*: NLCRIM was identical to LCRIM, but with no linguistic training.

B. Test Datasets

Three clothes-change data sets were used for the experiments. 1.) *Person Reidentification by Countour Sketch under Moderate Clothing Change (PRCC)* [40]. Images were captured across three cameras. Two cameras captured images in the same clothing set in different settings. The third camera captured images in different clothing sets on different days. 2.) *DeepChange* [39]. This set consists of 178k bounding boxes of 1.1k identities. Images are captured across 17

¹Earlier versions of LCRIM and NLCRIM were trained with substantially less data and without triplet loss hard negative mining [30].

TABLE I
TRAINING DATASETS

Dataset	Images	IDs	Clothes Change
UAV-Human [23]	41,290	119	no
MSMT17 [38]	29,204	930	no
Market1501 [45]	17,874	1,170	no
MARS [44]	509,914	625	no
STR-BRC [3]	156,688	224	yes
P-DESTRE [22]	214,950	124	no
PRCC [40]	17,896	150	yes
DeepChange [39]	28,1731	451	yes
BRS 1–5 [3]	697,348	995	yes
Total Training	1,966,895	4,788	

cameras from real-world surveillance systems and include changes in clothing as well as hairstyle. 3.) *HumanID* [31]. The HumanID dataset consists of videos of 297 identities filmed from multiple angles, viewpoints, and illumination conditions. We analyzed 94 of these identities. This subset had metadata for analysis of the camera angle.



Fig. 1. Sample images from the DeepChange dataset. Subject faces are blurred when visible according to DeepChange publication guidelines.

III. EXPERIMENTS AND RESULTS

A. Experiment 1—Face Contribution to Body Identification

In Part 1 of the experiment, we tested the models using body images with the face obscured. In Part 2, we tested the models using only the face. Bounding boxes for faces were found for the PRCC and HumanID dataset using a Multi-task Cascaded Convolutional Neural Network (MTCNN) trained to detect faces [42]. Images in which the detector failed to find a face were included in Part 1 and discarded for Part 2. The DeepChange dataset was excluded from both parts of Experiment 1, because faces were undetected in $\approx 97\%$ of the images, and because no faces were detected for certain identities, making face-based analyses impractical. Unless specified, input images were normalized using ImageNet means and standard deviations. Images were resized to 224×224 for LCRIM and NLCRIM and 384×384 for BIDDS and Swin-BIDDS.

1) *Part 1—Face Obscured*: Images in which faces were found were edited to place a black box over the face. The remaining images were left unchanged, under the assumption that no (or limited) facial information was available in these images. We calculated performance metrics (area under the ROC curve, AUC; mean average precision, mAP; Rank 1 and Rank 20 identification) on the modified datasets (black boxes drawn over faces found by MTCNN) and unmodified datasets (same images but with no transformations applied).

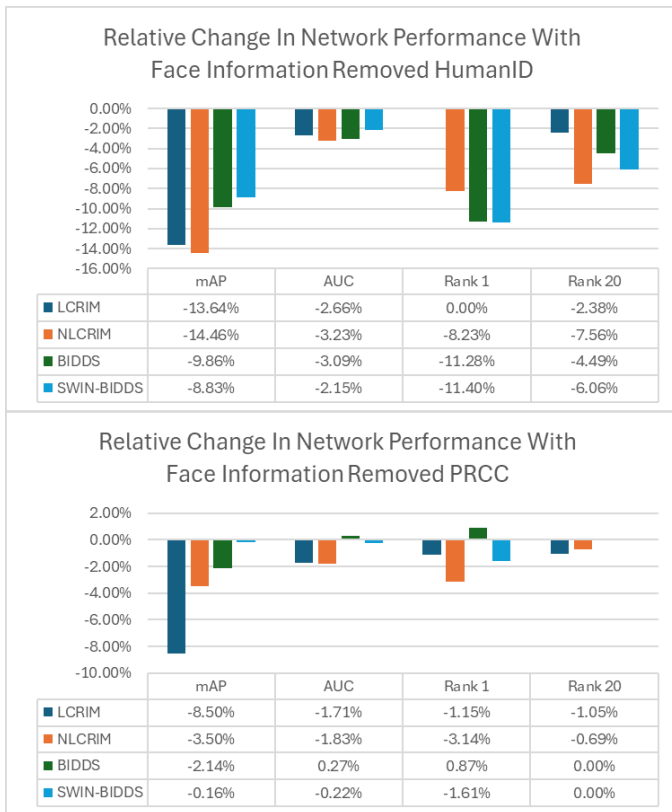


Fig. 2. The performance of the four body identification networks decreases when facial information is obscured.

Figure 2 shows that obscuring the face degrades identification accuracy for all models in both datasets, on most metrics. There was one exception: accuracy for the BIDDs model decreased only for mAP on the PRCC dataset. Performance dropped more on the challenging HumanID dataset than on the less challenging PRCC dataset. This suggests that the face may contribute relatively more to identification when the image quality overall is poor. The baseline accuracy of the four models was also a factor in performance when the face was obscured. The more accurate models overall (BIDDs, Swin-BIDDs) appeared to be more robust to the removal of facial information than the less accurate models (LCRIM, NLCRIM) (see Fig. 2). Without the face, metrics of matching accuracy such as Rank-1 and mAP declined more than AUC and Rank-20. This suggests that the face plays a key role in performing identity matching. These results demonstrate that identity-trained long-term body re-identification models utilize facial information when it is available—especially on challenging identification tasks.

2) *Part 2—Face Only*: Next, we tested the body-trained networks on cropped faces and compared identification accuracy with that of a high-performing facial identification network. To measure the baseline identification accuracy for the cropped faces (Face Baseline), we used a Controllable and Guided Face Synthesis for Unconstrained Face Recognition network, built on top of an ArcFace recognition module [25], [5]. This network was selected due to its strong performance on difficult unconstrained face identification datasets, such as IJB-B and IJB-C [29]. Consistent with the specified training

procedures ([25], [5]), images were normalized by mean = $[.5, .5, .5]$ and standard deviation = $[.5, .5, .5]$ and resized to 112x112 before being fed to the Face Baseline.

From the HumanID and PRCC datasets, two very challenging face datasets were constructed by cropping faces detected by MTCNN and replacing the original images with the cropped face images. Images in which a face was not found were discarded. The body identification networks were tested on these datasets, consisting only of cropped faces. Figure 3 shows example images.



Fig. 3. Sample cropped face images from the body dataset [31]. All subjects consented to publication.

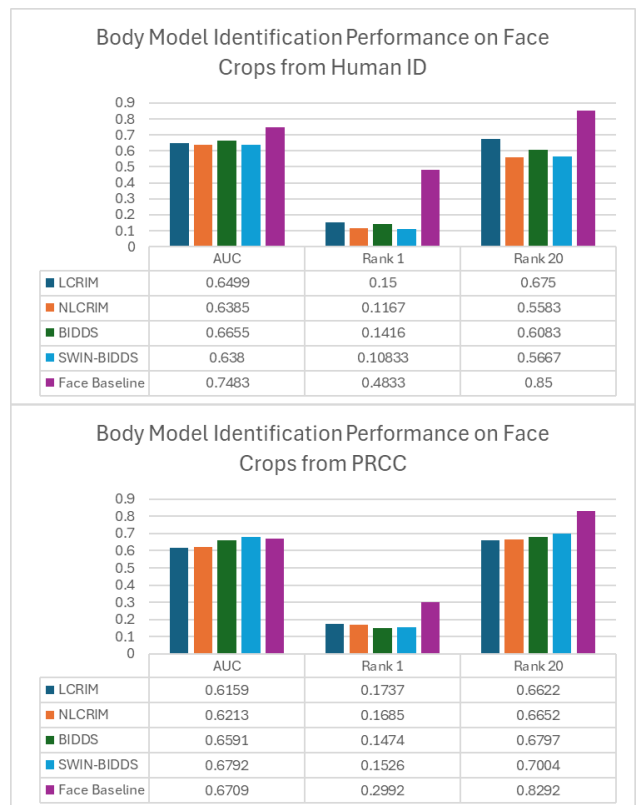


Fig. 4. Body networks learn residual information about face in their training. These networks can perform unconstrained face identification tasks to some degree.

The plots in Fig. 4 show that body re-identification networks learn useful information about faces. As expected, identification of these low quality faces from the body identification networks, overall, was far from perfect. However, relative to the face baseline network, performance is unexpectedly strong. For example, on the PRCC face data set, the AUC of the BIDDs model actually exceeded the baseline of the face-trained network. In all cases, AUC and rank 20 performance show that the body networks recognize faces with some degree of accuracy. As expected, rank 1 performance for all models, even the face baseline, is

low. This level of performance is appropriate given the image quality. Consistent with the face-obscured results, these findings suggest that body-trained identification models utilize information in the face.

Given the low quality of facial information in the HumanID and PRCC body-datasets, we constructed a test set from the popular (better quality) Labeled Faces in the Wild (LFW) face dataset [17]. Utilizing all identities that contain more than one image per identity, the test set contained 9,164 images of 1,680 identities, evenly split over a randomly assigned probe and gallery set. On this higher-quality face

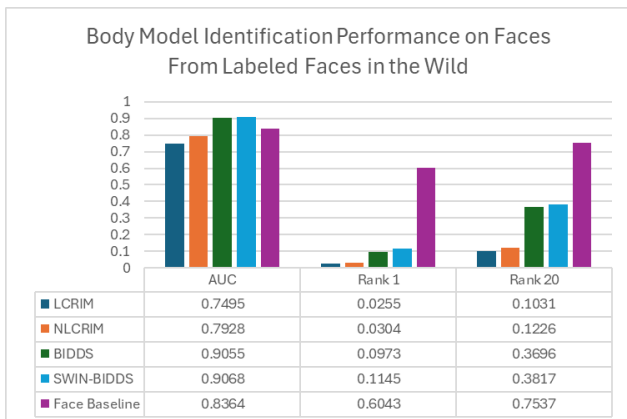


Fig. 5. Body Networks learn residual information about faces in their training. This information generalizes to high quality faces.

test, the body-identification models still perform better than expected with BIDDS and Swin-BIDDS surpassing the face baseline AUC. However, all body models perform substantially worse than the face baseline on retrieval tasks.

In summary, when the face was obscured, the stronger networks were more robust to the removal of face information. These networks also identified faces more accurately. Combined, the results suggest that the stronger person-identification networks use facial information more effectively when it is available, and depend less on the face when it is not available.

B. Experiment 2—Gender and Image Attribute Retention

In Part 1, we examine whether gender information is retained in body embeddings from the body identification networks. In Part 2, we examine the retention of image-specific information (viewpoint, dataset).

1) *Part 1—Gender*: Gender (male, female) was labeled manually for the PRCC, HumanID, and DeepChange datasets. Half of the identities from each dataset were randomly pooled into a single training set. The remaining identities comprised the test set. A logistic regression model was trained to predict gender from the image embeddings in the training set. The model was tested using the held-out image embeddings.

Figure 6 shows that the network embeddings retain information about gender. This is not entirely surprising, as gender serves as a useful discriminator when describing human bodies. Similar results have been reported for the analysis of face identification networks [15], [33], [34]. This

result is promising for future work with body-based GANS, which could utilize this semantic information as a basis for image editing.

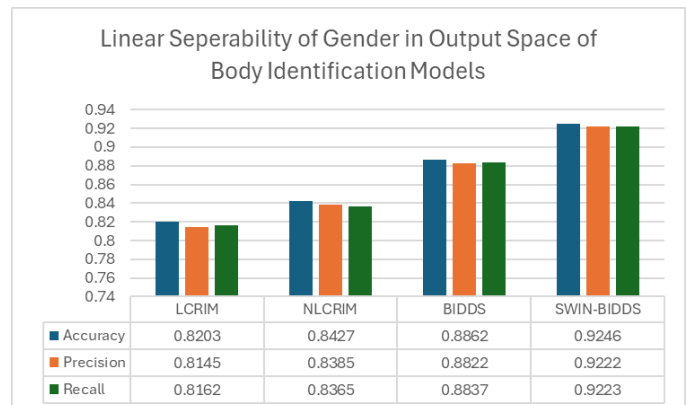


Fig. 6. Body network embeddings retain gender information which can be read out using linear models.

2) *Part 2—Image-based information*: We begin with the viewpoint, which is well-controlled and annotated in the HumanID dataset. This dataset provides body images from two viewpoints. These correspond to a person walking directly towards the camera (0° yaw) and walking perpendicular to the camera (90° yaw). From each viewpoint, a sequence of images was captured. These images were available for each person with two different clothing sets. A training set composed of embeddings from half of the images in the HumanID set was constructed; the remaining images were held out for testing. Again, logistic regression models were trained to predict the person’s yaw (0° vs. 90°) in the image.

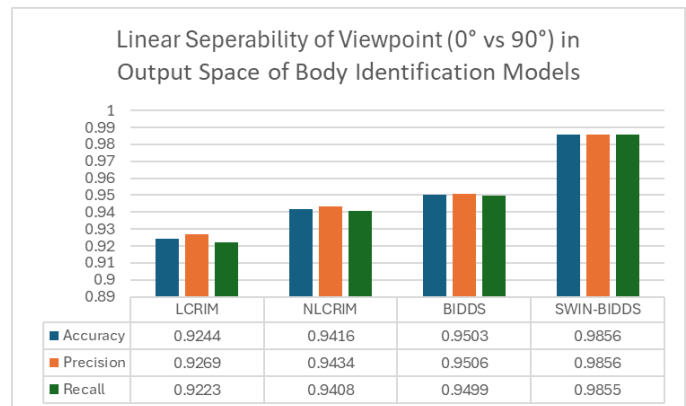


Fig. 7. Body network embeddings retain image viewpoint information which can be read out using linear models.

Figure 7 shows the results on the test set. All of the models retain information about the yaw of the person in the image. This finding is consistent with previous analyses for face networks [15]. Surprisingly, predictions of camera angle and gender demonstrate a relationship with model accuracy. Paradoxically, stronger person identification models seem to retain more non-identity information in their embeddings than weaker models.

Next, we asked whether the dataset of origin of the image could be predicted from the image embedding. Half of the identities from PRCC, HumanID, and DeepChange were

pooled into a training set. The remaining half of identities served as the test set. A logistic regression model was trained to predict dataset of origin. The embeddings corresponding to each image for each identity were input and the dataset of origin label was predicted.

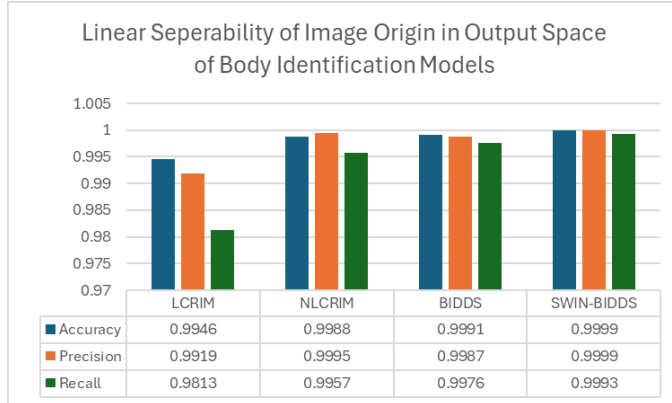


Fig. 8. Body network embeddings retain information pertaining to the origin of an image which can be read out using linear models.

Figure 8 shows that all models retain substantial information about the dataset from which an image was taken. This indicates that presumably trivial aspects of image quality, imaging conditions, or camera are retained in the embedding. Further experimentation is required to uncover exactly what information is retained to enable this prediction. Regardless, there are obvious potential applications in forensics and security for being able to trace image characteristics from a deep network embedding.

C. Experiment 3—Principal Component Analysis (PCA) and Dimensionality Reduction

1) *Part 1—Identification in PC Space*: In standard body identification tasks, image embeddings for gallery identities are compared to embeddings for probe identities. Here, we applied PCA to all gallery image embeddings. The original gallery embeddings X_g were then projected into the PC space yielding X_g^p . The probe set X_p was likewise projected into the PC space yielding X_p^p . Finally, performance metrics were calculated on X_g^p and X_p^p .

Table II shows that identification accuracy improves in the PCA space for all metrics and models, across the three datasets. There was only one exception—AUC for the Swin-BIDDS model on the DeepChange dataset declined slightly.

Performance boosts on average were modest, but highly consistent, and sometimes substantial. This shows that a computationally inexpensive and well-known technique that requires no additional training can be used to improve body identification accuracy.

2) *Part 2—Selective Dimensionality Reduction in PC Space*: First, we show that reducing the dimensionality of the PC space can lead to substantial performance increases for

²AUC and mAP metrics shown here are not comparable to those in Table II, because AUC is calculated on a templated gallery set. This distinction is made because this figure describes an approach that would be used in a re-identification system which would rely on templates.

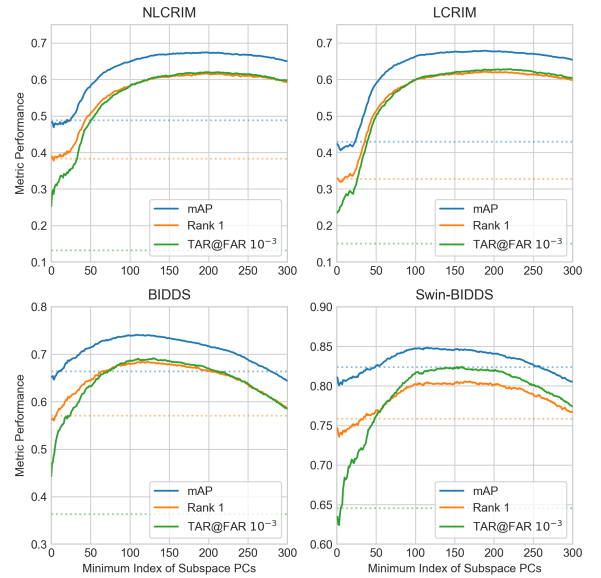


Fig. 9. *DeepChange Dataset*. Using an Oracle Algorithm to excise early principal components can lead to substantial boosts in Rank1, and TAR@FAR 10^{-3} , and mAP with some degradation in AUC (not shown). Horizontal lines indicate metric baselines from raw embeddings.²

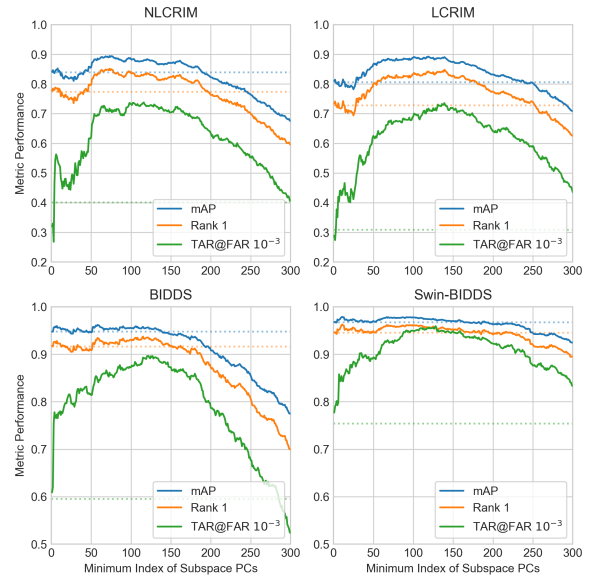


Fig. 10. *PRCC Dataset*. Using an Oracle Algorithm to excise early principal components can lead to substantial boosts in Rank1, TAR@FAR 10^{-3} , and mAP with some degradation in AUC (not shown). Horizontal lines indicate metric baselines from raw embeddings.²

our person-identification models. Dimensionality reduction was implemented by deleting the PCs that *explain the most variance* (cf. [32]) (i.e., delete PC_1 , then $PC_{1-2} \dots PC_{1-n}$). We begin with an “oracle simulation” that uses both probe and gallery items to implement dimensionality reduction. We then propose and test a method for dimensionality reduction that operates only on the gallery items, and can thereby be used in real-world applications. We show that this method achieves an appreciable performance increase.

The oracle method is described in Algorithm 1. We used network embeddings for each image in each dataset’s gallery ($X_{g,DeepChange}$, $X_{g,PRCC}$, and $X_{g,HumanID}$). Because $X_{g,PRCC}$, $X_{g,HumanID}$ contain a small number of identities

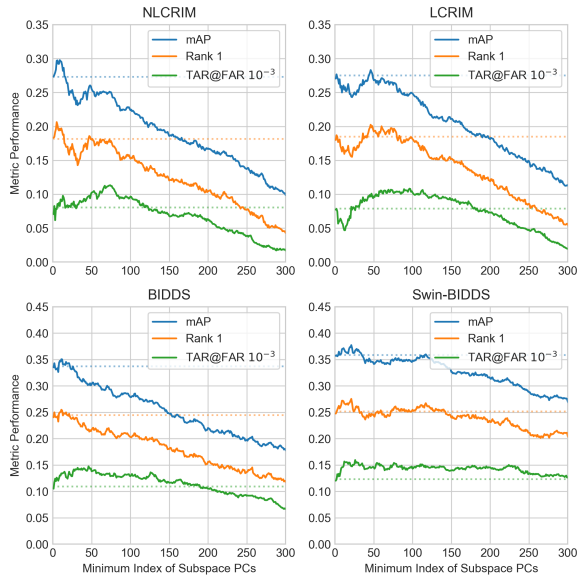


Fig. 11. *HumanID* Dataset. Using an Oracle Algorithm to excise early principal components can lead to modest boosts in Rank1, $TAR@FAR10^{-3}$, and mAP with some degradation in AUC (not shown). Horizontal lines indicate metric baselines from raw embeddings.²

Model	PCA	Dataset	MaP	AUC	ΔAUC	ΔMaP
LCRIM	No	DC	.1125	.7223	-	-
LCRIM	Yes	DC	.1189	.7385	$\uparrow 2.24\%$	$\uparrow 5.69\%$
NLCRIM	No	DC	.1537	.7462	-	-
NLCRIM	Yes	DC	.1625	.7695	$\uparrow 3.12\%$	$\uparrow 5.73\%$
BIDDS	No	DC	.2520	.7905	-	-
BIDDS	Yes	DC	.2583	.8062	$\uparrow 1.99\%$	$\uparrow 2.50\%$
SWIN-BIDDS	No	DC	.4325	.9210	-	-
SWIN-BIDDS	Yes	DC	.4339	.9153	$\uparrow 0.15\%$	$\downarrow 1.32\%$
LCRIM	No	PRCC	.4213	.8873	-	-
LCRIM	Yes	PRCC	.4646	.8939	$\uparrow 0.74\%$	$\uparrow 10.28\%$
NLCRIM	No	PRCC	.4882	.9030	-	-
NLCRIM	Yes	PRCC	.5093	.9128	$\uparrow 1.09\%$	$\uparrow 4.32\%$
BIDDS	No	PRCC	.6578	.9196	-	-
BIDDS	Yes	PRCC	.6817	.9417	$\uparrow 2.40\%$	$\uparrow 3.63\%$
SWIN-BIDDS	No	PRCC	.7020	.9390	-	-
SWIN-BIDDS	Yes	PRCC	.7147	.9495	$\uparrow 1.35\%$	$\uparrow 1.50\%$
LCRIM	No	H ID	.1261	.6963	-	-
LCRIM	Yes	H ID	.1557	.7326	$\uparrow 5.21\%$	$\uparrow 23.47\%$
NLCRIM	No	H ID	.1342	.7332	-	-
NLCRIM	Yes	H ID	.1574	.7615	$\uparrow 3.72\%$	$\uparrow 17.28\%$
BIDDS	No	H ID	.1907	.7706	-	-
BIDDS	Yes	H ID	.2192	.7910	$\uparrow 1.20\%$	$\uparrow 14.94\%$
SWIN-BIDDS	No	H ID	.2253	.8009	-	-
SWIN-BIDDS	Yes	H ID	.2566	.8192	$\uparrow 2.28\%$	$\uparrow 13.90\%$

TABLE II

PERFORMANCE COMPARISON ACROSS DEEPCHANGE (DC), PRCC, AND HUMANID (H ID) DATASETS WITH AND WITHOUT PCA APPLIED.

relative to the embedding space dimensionalities (71 and 94 respectively vs. 2048), a fourth gallery set was constructed $X_{g,all}$ by combining the gallery embeddings of the three datasets. This larger gallery supports the construction of informative PC representations.

Figs. 9 and 10 show the oracle results for DeepChange and PRCC, respectively. At a general level, the metrics follow an inverted U-shaped function as earlier PCs are progressively excised. Specifically, Rank 1, mAP, and $TAR@FAR10^{-3}$ increase substantially when earlier PCs are excised before classification. This peaks and declines when very large numbers of PCs are eliminated. For the HumanID dataset, Fig. 11 shows that Rank 1, mAP, and $TAR@FAR10^{-3}$ in-

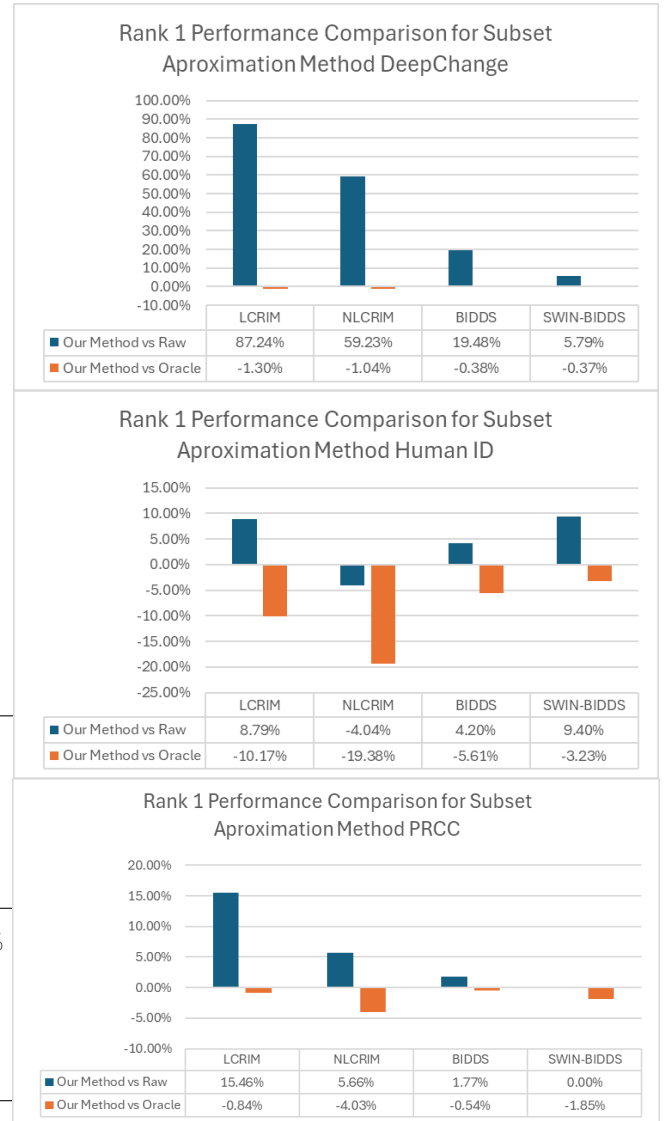


Fig. 12. Better subsets for rank 1 retrieval can be approximated with only the gallery set. Our method refers to performance achieved by algorithm 2, oracle refers to the optimal performance that can be achieved using algorithm 1, and raw refers to performance achieved by using unmodified network embeddings.

crease modestly before declining. Moreover, the performance peak occurs in much earlier principal components than for DeepChange and PRCC. This difference may arise from the difficult and small gallery available in HumanID. In summary, we show that across DeepChange, PRCC, and HumanID, eliminating early PCs *can* modestly boost and sometimes substantially boost multiple performance metrics.

Next, we propose and test a method for finding effective PC subspaces that can improve retrieval accuracy, based only on operations that use a pre-defined gallery set (see Algorithm 2). We test this on the three original (smaller) datasets. Here we focus on Rank 1 retrieval because it is most reflective of performance changes on small datasets like PRCC and HumanID. We compare our method to the use of the raw embeddings and to the oracle-selected embeddings.

Figure 12 shows that Rank 1 retrieval increases for the models on all datasets, with one exception: NLCRIM on the

HumanID Dataset when the PC subspace is utilized in place of unmodified embeddings. Performance increases vary according to dataset and model. On DeepChange, some models realize a near than 90% increase in Rank 1 performance. Comparatively, on HumanID the greatest increase in Rank 1 performance is 10%. Of note, the generally less performant models (e.g., LCRIM) show a larger benefit than the stronger models (BIDDS and SWIN-BIDDS). Also of note, Figure 12 shows that when using only a pre-defined gallery set, the performance of Algorithm 2 often approaches that of the oracle. Thus, using only a predefined gallery set, Algorithm 2 can substantially boost rank 1 retrieval, often nearly as well as an oracle algorithm.

In summary, excising early principal components from latent network representations consistently and often substantially boosts body identification network performance in both an oracle simulation and in a real world context.

Algorithm 1 Oracle Algorithm for Demonstrating the Effect of PC Subspaces on Identification Accuracy

- 1: **Input:** Network embeddings for Probe and Gallery sets X_p and X_g
 - 2: **Output:** PC subspaces and their corresponding identification metrics (mAP, Rank-1, TAR@FAR10⁻³)
 - 3: **Step 1: Construct Template Gallery ($X_{g,t}$):**
 - 4: **for** each identity in X_g **do**
 - 5: Compute the average of all embeddings for the given identity
 - 6: Add the averaged embedding as a template into $X_{g,t}$
 - 7: **end for**
 - 8: **Step 2: Compute PCA Basis:**
 - 9: Perform PCA on $X_{g,t}$
 - 10: Project $X_{g,t}$ and X_p into the PCA basis, yielding $X_{g,t}^{PCA}$ and X_p^{PCA}
 - 11: **Step 3: Order Principal Components:**
 - 12: Rank the eigenvectors of $X_{g,t}^{PCA}$ in descending order of explained variance
 - 13: **Step 4: Iterative Subspace Analysis:**
 - 14: **for** $k = 1$ to total number of eigenvectors **do**
 - 15: Remove the k largest eigenvectors (based on explained variance)
 - 16: Evaluate identification metrics (mAP, Rank-1, TAR@FAR10⁻³) using the subspace of $X_{g,t}^{PCA}$ and X_p^{PCA}
 - 17: **end for**
 - 18: **Return:** Return all evaluated subspaces and their corresponding identification metrics
-

IV. CONCLUSIONS AND FUTURE WORKS

A. Conclusions

This work provides an extensive analysis of four long-term person re-identification models. We show that facial information contributes to the performance of person re-identification models trained with whole-body images. Concomitantly, these models display a residual ability to identify

Algorithm 2 Subspace Approximation Method for Improving Accuracy

- 1: **Input:** Network embeddings for Probe and Gallery sets X_p and X_g
 - 2: **Output:** Modified embeddings for retrieval tasks
 - 3: **Step 1: Construct Template Gallery ($X_{g,t}$):**
 - 4: **for** each identity in X_g **do**
 - 5: Compute the average of all embeddings for the given identity
 - 6: Add the averaged embedding as a template into $X_{g,t}$
 - 7: **end for**
 - 8: **Step 2: Compute PCA Basis:**
 - 9: Perform PCA on $X_{g,t}$
 - 10: Project $X_{g,t}$, X_p , and X_g into the PCA basis, resulting in $X_{g,t}^{PCA}$, X_p^{PCA} , and X_g^{PCA}
 - 11: **Step 3: Subspace Search for Accuracy Improvement:**
 - 12: **for** each principal component **do**
 - 13: Remove the principal component with the highest explained variance
 - 14: Evaluate Rank-1 performance between $X_{g,t}^{PCA}$ and X_g^{PCA}
 - 15: **end for**
 - 16: **Step 4: Final Embedding Construction:**
 - 17: Identify the principal components corresponding to the highest Rank-1 performance between $X_{g,t}^{PCA}$ and X_g^{PCA}
 - 18: Remove these components from $X_{g,t}^{PCA}$ and X_p^{PCA} to create $X_{g,t}^{Final}$ and X_p^{Final}
 - 19: **Return:** $X_{g,t}^{Final}$ and X_p^{Final}
-

people using only the face. We demonstrate a number of parallels between body and face recognition models, with respect to their retention of information not relevant for identification. For example, the embeddings produced by body models include information about gender and camera angle, which can be linearly decoded from the network embeddings. Body networks also retain information about the dataset from which an image originated. In principle, this is consistent with the encoding of seemingly “trivial” image information, but it also opens the door to investigating exactly what information in the image can specify an originating dataset so accurately. We show that simple techniques previously used to boost identification performance are still applicable in the deep learning era. Finally, we provide an algorithm that substantially boosts our networks’ retrieval performance using only a pre-defined gallery set.

B. Future Works

The contribution of the face to body identification suggests opportunities for further improvement of face processing within the context of a whole person image. This could be done by training body networks to utilize face information more directly when it is available. Further experimentation on the types of image features that support image-origin predictions could open new security applications, such as tracking image sources. Additionally, exploring the information embedded in body network representations may reveal potential security risks associated with body identification

networks. In the dimensionality reduction experiment, we focused on removing early principal components. Future research could be aimed at identifying optimal PC subspaces.

V. ACKNOWLEDGMENTS

This research is based upon work supported in part by the Office of the Director of National Intelligence (ODNI), Intelligence Advanced Research Projects Activity (IARPA), via [2022-21102100005]. The views and conclusions contained herein are those of the authors and should not be interpreted as necessarily representing the official policies, either expressed or implied, of ODNI, IARPA, or the U.S. Government. The U.S. Government is authorized to reproduce and distribute reprints for governmental purposes notwithstanding any copyright annotation therein.

ETHICAL IMPACT STATEMENT

We have read the guidelines for the Ethical Impact Statement. The development of body identification models does not involve direct contact with human subjects, and therefore does not require approval by an Institutional Review Board. Instead, images/videos of human subjects are incorporated as training and test data for body identification models. We used only datasets (videos and images of people) that have been pre-screened and approved for ethical data collection standards by a United States government funding agency, XXXX. The standards applied for dataset approval require consent from the subjects who are depicted in the images/video for use in research. Images/videos of subjects who appear in publications require additional consent. We followed these guidelines carefully. Images displayed in the paper have been properly consented and are displayed according to the published instructions for use of the dataset.

The development and study of biometric identification algorithms entails risk to individuals and societies. It is clear that these systems can have negative impacts if they are misused. They can potentially threaten individual privacy and can impinge on freedom of movement and expression in a society. The goal of our work is to better understand how these systems function. The results of this work can have both positive and negative societal impacts. On the positive side, knowing the types of representations created by body identification networks can help to minimize person identification errors. It can also serve to set reasonable performance expectations, thereby limiting the scope of use. On the negative side, the knowledge gained can potentially be used to manipulate a system in unethical ways and to create synthetic images that can be misused or misinterpreted.

These risks are mitigated by the potential for positive societal impact. Body identification algorithms can be used

to locate missing people (including children). They can also be used in law enforcement to identify individuals implicated in crimes. Legitimate and societally-approved use can protect the general public from harm. Of note, body identification systems can be used in combination with face identification systems to improve identification accuracy, thereby minimizing erroneous identifications.

REFERENCES

- [1] J. Chen, X. Jiang, F. Wang, J. Zhang, F. Zheng, X. Sun, and W.-S. Zheng. Learning 3d shape feature for texture-insensitive person re-identification. In *Proceedings of the IEEE/CVF conference on computer vision and pattern recognition*, pages 8146–8155, 2021.
- [2] Y. I. Colón, C. D. Castillo, and A. J. O’Toole. Facial expression is retained in deep networks trained for face identification, 2021, in press.
- [3] D. Cornett, J. Brogan, N. Barber, D. Aykac, S. Baird, N. Burchfield, C. Dukes, A. Duncan, R. Ferrell, J. Goddard, et al. Expanding accurate person recognition to new altitudes and ranges: The briar dataset. In *Proceedings of the IEEE/CVF Winter Conference on Applications of Computer Vision*, pages 593–602, 2023.
- [4] K. Corona, K. Osterdahl, R. Collins, and A. Hoogs. Meva: A large-scale multiview, multimodal video dataset for activity detection. In *Proceedings of the IEEE/CVF Winter Conference on Applications of Computer Vision (WACV)*, pages 1060–1068, January 2021.
- [5] J. Deng, J. Guo, J. Yang, N. Xue, I. Kotsia, and S. Zafeiriou. Arcface: Additive angular margin loss for deep face recognition. *IEEE Transactions on Pattern Analysis and Machine Intelligence*, 44(10):5962–5979, Oct. 2022.
- [6] P. Dhar, A. Bansal, C. D. Castillo, J. Gleason, P. J. Phillips, and R. Chellappa. How are attributes expressed in face dcnns? In *2020 15th IEEE International Conference on Automatic Face and Gesture Recognition (FG 2020)*, pages 85–92, 2020.
- [7] J. Dietlmeier, J. Antony, K. McGuinness, and N. E. O’Connor. How important are faces for person re-identification? In *2020 25th International Conference on Pattern Recognition (ICPR)*, pages 6912–6919. IEEE, 2021.
- [8] A. Dosovitskiy, L. Beyer, A. Kolesnikov, D. Weissenborn, X. Zhai, T. Unterthiner, M. Dehghani, M. Minderer, G. Heigold, S. Gelly, J. Uszkoreit, and N. Houlsby. An image is worth 16x16 words: Transformers for image recognition at scale, 2021.
- [9] K. Etemad and R. Chellappa. Discriminant analysis for recognition of human face images. *J. Opt. Soc. Am. A*, 14(8):1724–1733, Aug 1997.
- [10] A. A. Gharbi, A. Chouchane, A. Ouamane, and M. Bessaoudi. Advancing person re-identification: Tensor-based feature fusion and multilinear subspace learning. In *2024 8th International Conference on Image and Signal Processing and their Applications (ISPA)*, pages 1–7, 2024.
- [11] I. Goodfellow, J. Pouget-Abadie, M. Mirza, B. Xu, D. Warde-Farley, S. Ozair, A. Courville, and Y. Bengio. Generative adversarial networks. *Communications of the ACM*, 63(11):139–144, 2020.
- [12] X. Gu, H. Chang, B. Ma, S. Bai, S. Shan, and X. Chen. Clothes-changing person re-identification with rgb modality only. In *Proceedings of the IEEE/CVF conference on computer vision and pattern recognition*, pages 1060–1069, 2022.
- [13] K. He, X. Zhang, S. Ren, and J. Sun. Deep residual learning for image recognition, 2015.
- [14] A. Hermans, L. Beyer, and B. Leibe. In defense of the triplet loss for person re-identification. *arXiv preprint arXiv:1703.07737*, 2017.
- [15] M. Q. Hill, C. J. Parde, C. D. Castillo, Y. I. Colon, R. Ranjan, J.-C. Chen, V. Blanz, and A. J. O’Toole. Deep convolutional neural networks in the face of caricature. *Nature Machine Intelligence*, 1(11):522–529, 2019.
- [16] P. Hong, T. Wu, A. Wu, X. Han, and W.-S. Zheng. Fine-grained shape-appearance mutual learning for cloth-changing person re-identification.

- In *Proceedings of the IEEE/CVF conference on computer vision and pattern recognition*, pages 10513–10522, 2021.
- [17] G. B. Huang, M. Mattar, T. Berg, and E. Learned-Miller. Labeled faces in the wild: A database for studying face recognition in unconstrained environments. In *Workshop on faces in 'Real-Life' Images: detection, alignment, and recognition*, 2008.
- [18] S. Huang, R. P. Kathirvel, C. P. Lau, and R. Chellappa. Whole-body detection, recognition and identification at altitude and range, 2023.
- [19] H. Jégou and O. Chum. Negative evidences and co-occurrences in image retrieval: The benefit of pca and whitening. In A. Fitzgibbon, S. Lazebnik, P. Perona, Y. Sato, and C. Schmid, editors, *Computer Vision – ECCV 2012*, pages 774–787, Berlin, Heidelberg, 2012. Springer Berlin Heidelberg.
- [20] D. P. Kingma and J. Ba. Adam: A method for stochastic optimization, 2017.
- [21] J. Križaj, R. O. Plesh, M. Banavar, S. Schuckers, and V. Štruc. Deep face decoder: Towards understanding the embedding space of convolutional networks through visual reconstruction of deep face templates. *Engineering Applications of Artificial Intelligence*, 132:107941, 2024.
- [22] S. A. Kumar, E. Yaghoubi, A. Das, B. Harish, and H. Proença. The p-destre: A fully annotated dataset for pedestrian detection, tracking, and short/long-term re-identification from aerial devices. *IEEE Transactions on Information Forensics and Security*, 16:1696–1708, 2020.
- [23] T. Li, J. Liu, W. Zhang, Y. Ni, W. Wang, and Z. Li. Uav-human: A large benchmark for human behavior understanding with unmanned aerial vehicles. In *2021 IEEE/CVF Conference on Computer Vision and Pattern Recognition (CVPR)*, pages 16261–16270, 2021.
- [24] F. Liu, M. Kim, Z. Gu, A. Jain, and X. Liu. Learning clothing and pose invariant 3d shape representation for long-term person re-identification. In *Proceedings of the IEEE/CVF International Conference on Computer Vision*, pages 19617–19626, 2023.
- [25] F. Liu, M. Kim, A. Jain, and X. Liu. Controllable and guided face synthesis for unconstrained face recognition, 2022.
- [26] F. Liu, M. Kim, Z. Ren, and X. Liu. Distilling clip with dual guidance for learning discriminative human body shape representation. In *Proceedings of the IEEE/CVF Conference on Computer Vision and Pattern Recognition (CVPR)*, pages 256–266, June 2024.
- [27] Z. Liu, Y. Lin, Y. Cao, H. Hu, Y. Wei, Z. Zhang, S. Lin, and B. Guo. Swin transformer: Hierarchical vision transformer using shifted windows, 2021.
- [28] Z. Liu, Y. Lin, Y. Cao, H. Hu, Y. Wei, Z. Zhang, S. Lin, and B. Guo. Swin transformer: Hierarchical vision transformer using shifted windows. In *Proceedings of the IEEE/CVF international conference on computer vision*, pages 10012–10022, 2021.
- [29] B. Maze, J. Adams, J. A. Duncan, N. Kalka, T. Miller, C. Otto, A. K. Jain, W. T. Niggel, J. Anderson, J. Cheney, et al. Iarpa janus benchmark-c: Face dataset and protocol. In *2018 international conference on biometrics (ICB)*, pages 158–165. IEEE, 2018.
- [30] B. A. Myers, L. Jaggernauth, T. M. Metz, M. Q. Hill, V. N. Gandhi, C. D. Castillo, and A. J. O’Toole. Recognizing people by body shape using deep networks of images and words. *Proceedings of the IEEE: International Joint Conference on Biometrics*, 2023.
- [31] A. O’Toole, J. Harms, S. Snow, D. Hurst, M. Pappas, J. Ayyad, and H. Abdi. A video database of moving faces and people. *IEEE Transactions on Pattern Analysis and Machine Intelligence*, 27(5):812–816, 2005.
- [32] A. J. O’Toole, H. Abdi, K. A. Deffenbacher, and D. Valentin. Low-dimensional representation of faces in higher dimensions of the face space. *Journal of the Optical Society of America A*, 10(3):405–411, 1993.
- [33] C. J. Parde, C. Castillo, M. Q. Hill, Y. I. Colon, S. Sankaranarayanan, J.-C. Chen, and A. J. O’Toole. Face and image representation in deep cnn features. In *Automatic Face & Gesture Recognition (FG 2017), 2017 12th IEEE International Conference on*, pages 673–680. IEEE, 2017.
- [34] C. J. Parde, Y. I. Colón, M. Q. Hill, C. D. Castillo, P. Dhar, and A. J. O’Toole. Closing the gap between single-unit and neural population codes: Insights from deep learning in face recognition. *Journal of vision*, 21(8):15–15, 2021.
- [35] O. Russakovsky, J. Deng, H. Su, J. Krause, S. Satheesh, S. Ma, Z. Huang, A. Karpathy, A. Khosla, M. Bernstein, et al. Imagenet large scale visual recognition challenge. *International journal of computer vision*, 115:211–252, 2015.
- [36] Y. Shen, J. Gu, X. Tang, and B. Zhou. Interpreting the latent space of gans for semantic face editing. In *Proceedings of the IEEE/CVF conference on computer vision and pattern recognition*, pages 9243–9252, 2020.
- [37] P. Terhörst, D. Fährmann, N. Damer, F. Kirchbuchner, and A. Kuijper. Beyond identity: What information is stored in biometric face templates? *arXiv preprint arXiv:2009.09918*, 2020.
- [38] L. Wei, S. Zhang, W. Gao, and Q. Tian. Person transfer gan to bridge domain gap for person re-identification. In *Proceedings of the IEEE conference on computer vision and pattern recognition*, pages 79–88, 2018.
- [39] P. Xu and X. Zhu. Deepchange: A long-term person re-identification benchmark with clothes change. In *Proceedings of the IEEE/CVF International Conference on Computer Vision*, pages 11196–11205, 2023.
- [40] Q. Yang, A. Wu, and W.-S. Zheng. Person re-identification by contour sketch under moderate clothing change. *IEEE transactions on pattern analysis and machine intelligence*, 43(6):2029–2046, 2019.
- [41] M. Ye, J. Shen, G. Lin, T. Xiang, L. Shao, and S. C. Hoi. Deep learning for person re-identification: A survey and outlook. *IEEE transactions on pattern analysis and machine intelligence*, 44(6):2872–2893, 2021.
- [42] K. Zhang, Z. Zhang, Z. Li, and Y. Qiao. Joint face detection and alignment using multitask cascaded convolutional networks. *IEEE Signal Processing Letters*, 23(10):1499–1503, Oct. 2016.
- [43] W. Zhao, A. Krishnaswamy, R. Chellappa, D. L. Swets, and J. Weng. *Discriminant Analysis of Principal Components for Face Recognition*, pages 73–85. Springer Berlin Heidelberg, Berlin, Heidelberg, 1998.
- [44] L. Zheng, Z. Bie, Y. Sun, J. Wang, C. Su, S. Wang, and Q. Tian. Mars: A video benchmark for large-scale person re-identification. In *Computer Vision–ECCV 2016: 14th European Conference, Amsterdam, The Netherlands, October 11–14, 2016, Proceedings, Part VI 14*, pages 868–884. Springer, 2016.
- [45] L. Zheng, L. Shen, L. Tian, S. Wang, J. Wang, and Q. Tian. Scalable person re-identification: A benchmark. In *Proceedings of the IEEE international conference on computer vision*, pages 1116–1124, 2015.